



Lawrence Berkeley Laboratory

UNIVERSITY OF CALIFORNIA

Materials & Molecular Research Division

Submitted to the Journal of Physical Chemistry

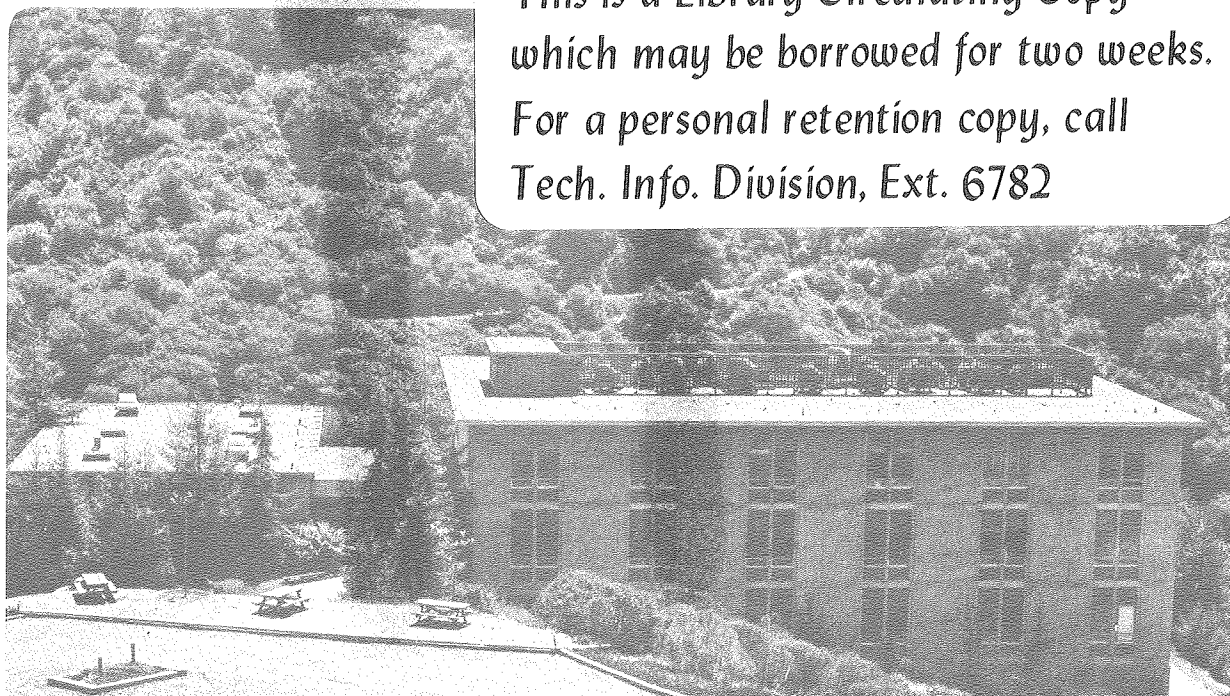
ADSORPTION AND BONDING OF BUTANE AND PENTANE ON THE
Pt(111) CRYSTAL SURFACES. EFFECTS OF OXYGEN TREATMENTS
AND DEUTERIUM PREADSORPTION

M. Salmerón and G.A. Somorjai

April 1981

TWO-WEEK LOAN COPY

*This is a Library Circulating Copy
which may be borrowed for two weeks.
For a personal retention copy, call
Tech. Info. Division, Ext. 6782*



LBL-12617
c. 2

DISCLAIMER

This document was prepared as an account of work sponsored by the United States Government. While this document is believed to contain correct information, neither the United States Government nor any agency thereof, nor the Regents of the University of California, nor any of their employees, makes any warranty, express or implied, or assumes any legal responsibility for the accuracy, completeness, or usefulness of any information, apparatus, product, or process disclosed, or represents that its use would not infringe privately owned rights. Reference herein to any specific commercial product, process, or service by its trade name, trademark, manufacturer, or otherwise, does not necessarily constitute or imply its endorsement, recommendation, or favoring by the United States Government or any agency thereof, or the Regents of the University of California. The views and opinions of authors expressed herein do not necessarily state or reflect those of the United States Government or any agency thereof or the Regents of the University of California.

ADSORPTION AND BONDING OF BUTANE AND PENTANE ON
THE Pt(111) CRYSTAL SURFACES. EFFECTS OF OXYGEN TREATMENTS
AND DEUTERIUM PREADSORPTION

M. Salmerón* and G.A. Somorjai

Materials and Molecular Research Division, Lawrence Berkeley Laboratory
and
Department of Chemistry, University of California, Berkeley, CA 94720

Abstract

The adsorption of C_4H_{10} and C_5H_{12} on Pt(111) was studied by thermal desorption spectroscopy. Both hydrocarbons show a first order desorption process with peak temperatures of 166° and 195°K. Kinetic parameters obtained were $\nu = 9.4 \times 10^{10} \text{sec}^{-1}$, $E = 8.2 \text{ kcal/mol}$, and $\nu = 3.7 \times 10^{11} \text{sec}^{-1}$, $E = 10.2 \text{ kcal/mol}$ for C_4H_{10} and C_5H_{12} , respectively. Multilayers of both hydrocarbons are formed at 110°K and high exposures. The presence of subsurface oxygen introduces new adsorption sites and decreases the exposure needed for multilayer formation. Preadsorbed deuterium interacts repulsively with the adsorbed hydrocarbons, lowering its desorption temperature.

This work was supported by the Director, Office of Energy Research,
Office of Basic Energy Sciences, Materials Sciences Division of the
U.S. Department of Energy under Contract W-7405-ENG-48;
and the Spanish-American Cooperation Program.

*Permanent address: Instituto de Física del Estado Sólido,
Universidad Autónoma de Madrid,
Cantoblanco, Madrid, Spain

Introduction

The adsorption characteristics (heats of adsorption, monolayer structure, surface sensitivity, and bonding) of alkanes on metal surfaces are an important area of investigation for many reasons. Alkanes are often reactants in hydrocarbon conversion reactions leading to the production of olefins and cyclic hydrocarbons. They are also major constituents of lubricants, adhesives, and other surface active agents where the molecular scale bonding properties to the solid surface determine their utility. The use of single crystals for adsorption studies permits precise control of the surface structure which can markedly influence the nature of the chemical bonds between the organic adsorbates and the solid substrates as demonstrated by many recent studies.¹

We have investigated the adsorption characteristics of butane and pentane on the (111) crystal face of platinum. These molecules are considered representative of the larger class of alkanes C_nH_{2n+2} , and it was thought that their behavior will be reflected in the behavior of other molecules in this class of compounds. The Pt(111) surface was chosen for many reasons. Firment *et al.*² studied the surface structure of alkanes by low energy electron diffraction (LEED) on this crystal face and determined the ordering and growth characteristics of alkane monolayers and films. We could then utilize this knowledge to obtain a more complete picture of the nature of their bonding.

The adsorption studies were carried out in the temperature range of 110-800°K. Thermal desorption spectroscopy (TDS) was used to obtain heats of desorption. The influence of preadsorbed deuterium and oxygen was also studied since these adsorbates that are often ingredients in the catalyzed surface reactions of alkanes markedly influence the adsorption characteristics.

2. Experimental

The experiments were performed in a ultrahigh vacuum chamber evacuated with ion and diffusion pumps. The Pt(111) samples were in the form of thin discs of approximately 1 cm diameter and a thickness of ~ 1 mm. The crystal was mounted on a U-shaped platinum wire of 0.020 inch diameter, spot welded around the edges. Temperatures were measured by means of a chromel-alumel thermocouple spot welded to the top edge of the crystal. Heat was carried to and from the crystal through the Pt wires. These wires were firmly fastened to two copper blocks that were cooled to liquid nitrogen temperatures. The crystal could also be rotated to allow monitoring for Auger spectrometry (AES), and thermal desorption experiments (TDS). Detection of the various desorption products was performed with a UTI mass spectrometer with the ionizer placed at approximately 10 cm from the Pt crystal face. A linear temperature ramp was achieved in the range 110-800° K by suddenly passing a high current of the order of 15 amps through the supporting Pt wires. The heating rates were always in the range of 7-14°K/sec, with a constancy of $\pm 0.5^\circ\text{K}/\text{sec}$. in the said temperature range. Pumping times for the different gases used were of the order of 0.5 seconds.

The different hydrocarbons used in this work were introduced into the vacuum chamber via a leak valve with a capillary tube to dose the crystal from approximately 1 cm distance from its surface. Pressures and exposures were measured with a Bayard-Alpert ion gauge without correction for inhomogeneous pressure distributions and for difference in sensitivity, especially with hydrocarbons. The values of all the exposures in Langmuirs ($1 \text{ L} = 10^{-6}$ Torr x sec) given in this work are thus only qualitative.

The cleanliness of the surface was monitored by Auger electron spectroscopy (AES) with a retarding field analyzer. Carbon could be easily removed by heating in 2×10^{-7} Torr of O_2 for 5-10 minutes at a crystal temperature of approximately $1000^\circ K$. Subsequently the crystal was flashed to above $1300^\circ K$ and then cooled to $110^\circ K$ in a period of approximately five minutes.

Background pressures in the range of 10^{-10} Torr were usually obtained, but increased during the course of hydrocarbon adsorption to reach a final value between 1 and 2×10^{-9} Torr. It is possible, however, that this background pressure is inhomogeneous as the LN cooling device near the crystal acted as a very effective cryopump.

3. Results

3.1 Butane. At the lowest Pt crystal temperature that would be reached close to $110^\circ K$, only the alkanes C_nH_{2n+2} , with $n > 4$, could be adsorbed on the surface. Butane adsorbed readily at $110^\circ K$ and desorbed without decomposition. The TDS curves corresponding to various exposures are shown in Figure 1. For exposures of less than 0.5 L, one major peak is observed at $T = 166^\circ K \pm 2^\circ K$. The area under this peak grows linearly with exposure up to 0.5 L where saturation occurs, as shown in the insert of Figure 1.

The temperature at which the desorption peak appears was found to be independent of coverage, indicating first order desorption. This is also indicated by the observed asymmetry of the peak with a long tail at the low temperature side and a rapid fall-off of the high temperature tail. The temperatures corresponding to the half peak heights are $157^\circ K$ and $173^\circ K$. At higher exposures, a broad desorption peak appears below approximately $150^\circ K$ which increases rapidly initially and at a slower rate for exposures larger than 2 L. This is also shown in the insert of Figure 1.

Butane was also adsorbed on an oxygen pretreated Pt(111) surface. The treatment consisted in prolonging the carbon O₂ cleaning procedure at 1100°K until after evacuating the gas phase O₂ and flashing again to 1100°K an oxygen peak was detected in the Auger spectrum. In the experiments displayed in Figure 2, the ratio of oxygen to platinum Auger peak heights (O/Pt₂₃₇) was 0.4. The TDS curves from adsorbed C₄H₁₀ are shown in this figure for various hydrocarbon exposures. At low exposures a broad peak with a maximum at 166°K is observed. Several other peaks are also clustering around this temperature that grow larger for higher exposures. Peak temperatures are observed at 163°K, 148°K, and 134°K. Their presence indicates a heterogeneous surface, offering a variety of adsorption sites to the C₄H₁₀ molecules. At exposures above 0.2 L, the peak at 134°K increases rapidly and linearly with exposure which indicates the formation of multilayers. It is interesting to note that in the oxygen treated surface the growth of C₄H₁₀ layers occurs at lower exposures than those required on the clean surface. The insert in Figure 2 shows the increase in the area of the various peaks in the TDS curves as a function of exposure. If D₂ was preadsorbed on this Pt surface, it was found that subsequent C₄H₁₀ adsorption showed an increased peak at 134°K, as shown in the dotted TDS curve of Figure 2, which corresponds to a D₂ exposure of 0.5 L, followed by approximately 0.2 L of C₄H₁₀. The intensity of the 134°K peak depends on the D₂ exposure. This result is also in agreement with the observed sensitivity of this multilayer desorption peak to H₂ adsorption from the background.

3.2 Pentane. A study similar to the one described above for C₄H₁₀ was performed with C₅H₁₂. The TDS curves for various exposures are shown in Figure 3. At exposures below 0.3 L, a major peak is observed at $195 \pm 2^\circ\text{K}$, that increases linearly with exposure up to saturation. The asymmetry of this peak, with half-peak height temperatures of 185 and 203 K and its invariance with coverage (below 0.3 L) indicates that it corresponds to a first order

desorption process. Another broad peak appears at approximately 153 K. This peak grows at exposures above 0.3 L and a multitude of other peaks appear also at these higher exposures. The peak temperatures are 187°, 157°, and 137°K. The 195°K peak appears to shift at these high exposures to a temperature of 204 K. However, the general behavior is similar to that of butane.

If the exposure is increased above 1.3 L, a new sharp peak at 125 K appears that grows indefinitely with exposure indicating the formation of multilayers. In Figure 4 we show the variation of the total area under the TDS curves versus exposure. For the 195°K peak, the area at exposures larger than 0.3 L was estimated by measuring the height of the peak and assuming the same width as in the low exposure curves.

The effect of oxygen treatments was also investigated in this case. Experiments corresponding to a ratio of Auger peak heights $O/Pt_{237} \approx 0.1$ are shown in Figure 5. Two peaks are visible at low exposures and up to 0.4 L approximately. The low temperature peak appears initially at 130°K and then apparently shifts to higher temperatures as a result of its overlap with another low temperature peak that shows up clearly only above 0.4 L. The peak at 195°K shows a behavior similar to that in the clean surface. At even higher exposures, i.e. above 1 L, multilayer formation occurs as shown by the unlimited increase of the peaks at 129° and 135°K.

Finally, C_5H_{12} was adsorbed on a D_2 precovered surface. In a first experiment, the adsorption of D_2 alone was studied at 110 K in order to estimate the coverages.

The plot of Figure 6 was obtained by measuring the area under the D_2 TDS curves. The value of $\theta = 1$ was assigned to what seems to correspond to satura-

tion, i.e. to an area of 4 in the arbitrary units of Figure 6. Pentane was then adsorbed on the surface with various amounts of preadsorbed deuterium. A set of TDS curves corresponding to 0.1 L of C_5H_{12} is shown in Figure 7. We observe a shift in the position of the 195°K peak toward lower temperatures with increasing deuterium exposure. This shift is plotted in Figure 8 versus D-coverage obtained using the data of Figure 6. Data corresponding to 0.6 L of C_5H_{12} are also shown. Another effect of preadsorbed deuterium is to favor the formation of multilayers at hydrocarbon exposures lower than the ones necessary for the clean surface.

If in these coadsorption experiments the mass spectrometer was tuned to the atomic mass unit 4, the observed TDS curves did not differ in shape, area or position from those obtained with D_2 alone. In another experiment, a surface covered with 0.3 L of C_5H_{12} was then exposed to D_2 . No adsorption of D_2 was observed to occur in that case, however. Exchange of H and D between the coadsorbed paraffin and adsorbed D was not observed either.

4. Discussion

4.1 Butane. The constant peak temperature of the C_4H_{10} TDS curves for all coverages indicates that the desorption process is first-order. This is also consistent with the asymmetry of the peak with a longer low temperature tail (see experimental section), as expected from a first-order process. Since high pumping speeds and low heating rates³ were used in our experiments, the classical treatment of thermal desorption spectra can be applied.⁴⁻⁶ The observed pressure increase, P, is proportional to the rate of desorption:

$$P = -C \frac{dn}{dt} = C \nu n e^{-E/RT}$$

where C is a constant containing the pumping speed, volume of the chamber, etc., n is the concentration of surface species, and ν and E are the preexponential and activation energies for the desorption process. This equation can be solved to yield

$$P = C n_0 \nu \exp \left\{ \frac{-E}{RT} - \frac{\nu}{\beta} \int_{T_0}^T \exp\left(-\frac{E}{RT}\right) dT \right\} \quad (1)$$

with n_0 being the initial surface concentration of adsorbed hydrocarbon. T_0 and β are the initial temperature and heating rate, respectively.

When trying to fit Eq.1 to the experimental curves, we find that only the low or high temperature tail could be matched for a pair of ν , E values satisfying the condition of peak maximum:⁴

$$\frac{E}{RT_m^2} = \frac{\nu}{\beta} e^{E/RT_m} \quad \text{where } T_m \text{ is the temperature of the peak, i.e.}$$

166°K for C_4H_{10} . This result is not surprising in view of the broadening of the TDS curve that arises from small variations of E and ν across the surface of the crystal due to heterogeneities and also to inhomogeneous temperature distributions across the crystal. Since this broadening affects more strongly the rapidly varying high temperature tail, we have chosen the E and ν values that gave the best fit with the low temperature tail. In particular, the optimization procedure used was to reproduce the experimental width, measured from the low temperature half-maximum, 157°K, to the peak maximum, 166°K. The values so obtained were $\nu = 9.4 \times 10^{10} \text{sec}^{-1}$ and $E = 8.2 \text{ kcal/mol}$. The fit between the calculated curve (Eq.1) and the experimental one is similar to that shown in Figure 3b for the case of C_5H_{12} to be discussed later.

At exposures above .3 L, an increase in the area under the TDS curve is observed (Figure 1), while the intensity of the peak at 166°K remains constant. This corresponds to adsorption on lower binding energy sites. The saturation of the sites, at exposures of the order of 2 L, yields a total area a little larger than twice that corresponding to the first peak alone, as shown in the insert of Figure 1.

In a LEED study of the adsorption of paraffins on Pt(111), Firment et al.² observed three different structures corresponding to different exposures of C₄H₁₀. In the temperature range studied here, only two of these structures are formed. The low exposure one, showing a LEED pattern of $\begin{pmatrix} 2 & 5 \\ 2 & -5 \end{pmatrix}$ symmetry, has four molecules per unit cell and a packing of 33.4 Å²/molecule. According to these authors, this packing corresponds to molecules lying flat on the surface and separated by their Van der Waals radii. The high exposure structure, with a symmetry $\begin{pmatrix} 3 & -2 \\ 2 & 5 \end{pmatrix}$ corresponds to a denser packing of 31.6 Å²/molecule. The authors suggest that the hydrocarbon molecules have their long axis no longer parallel to the surface. In view of our data, it is tempting to associate the growth of the peak at 166°K to the formation of the first structure, while after saturation of this peak the second structure forms, corresponding to the filling of the lower binding energy sites.

On the oxygen treated surface, the appearance of new peaks at lower temperatures can be associated with adsorption on oxide patches. In a recent study⁷ we have shown that the distribution of subsurface oxygen is inhomogeneous and gives rise to various ordered LEED structures. Apart from providing new adsorption sites, the presence of this subsurface oxygen facilitates the formation of multilayers, as shown in Figure 2, that could not be formed on the clean surface at ~ 110°K for exposures below 2 L. This effect may be explained by the rapid saturation of the high binding energy sites associated with clean Pt patches. The same explanation can be applied to the case of D₂ preadsorption that would decrease again the number of available high binding energy sites.

4.2 Pentane. The same analysis employed for butane can be applied to the major TDS peak of C_5H_{12} at $195^\circ K$. The best fit of Eq. 1 to the experimental curves, using the width from the low temperature half-maximum, 185 K, to the peak temperature, 195K, as optimizing criterion, yielded the values $\nu = 3.7 \times 10^{11} \text{sec}^{-1}$ and $E = 10.2 \text{ kcal/mol}$. An example of the fit obtained using these values is shown in Figure 3b.

As in the case of C_4H_{10} , the saturation of the low exposure peak at $195^\circ K$ is followed by the filling up of lower binding energy sites. The total area in Figure 4 is shown to be 3.5 times larger at the saturation of the monolayer than that of the $195^\circ K$ peak alone. This observation could be explained if, as in the case of C_4H_{10} , the molecules are packed with their long axis inclined with respect to the Pt(111) surface at the higher coverages.

In the O_2 pretreated surface the oxide patches cause the appearance of a peak around $130^\circ K$ that grows to multilayer thickness at exposures below the ones corresponding to multilayer formation on the clean surface. The multilayer desorption shows two peaks at $129^\circ K$ and $135^\circ K$, not very different from the $125^\circ K$ observed on the clean surface. The higher temperature peaks are much the same as those from the corresponding clean surface, consistent with the coexistence of patches of clean and oxidized regions.

4.3 The Effect of D_2 Preadsorption. The adsorption of C_4H_{10} and C_5H_{12} on a D_2 covered surface results in the more facile formation of multilayers of hydrocarbon. On a partially deuterated surface, the hydrocarbon may be

thought to fill up first the free metal sites unaffected by deuterium adsorption, and then adsorb on the hydrocarbon islands, forming multilayers. The build-up of these multilayers will start then at lower exposures than in the case of clean surfaces.

The results of Figures 7 and 8 show a shift in the desorption temperature of C_5H_{12} as a function of deuterium exposure. In Figure 8 the vertical temperature scale has been converted to activation energies obtained from a fit of Eq.1 to the experimental low temperature half-width in the manner explained above. A slow decrease in the activation energy, E , is observed as a function of coverage θ , up to θ values between 0.8 and 0.9. For higher coverages, a much more rapid decrease of E is observed.

The decrease, at first, may be due to hydrocarbon adsorbing on the clean Pt surface. As adsorption proceeds, repulsive interactions between the adsorbed hydrocarbon and deuterium atoms gives rise to a decrease in the desorption peak temperature until at large coverages the hydrocarbon is forced to adsorb on top of the deuterium layer which would result in a more rapid decrease in the apparent binding energy. Although the same effects of shifts to lower temperatures should occur for the desorption of D_2 , according to the repulsive interaction mentioned, it is not observable with these two paraffins as D_2 desorbs at much higher temperatures ($\sim 300^\circ K$), when the paraffin has already desorbed. In fact, the desorption curves for D_2 adsorbed on Pt with or without alkane coadsorption are identical. With other hydrocarbons of higher desorption temperatures and, therefore, stronger bonding to the metal surface as the unsaturated hydrocarbons, the D_2 TDS curves peak at temperatures much

lower than those corresponding to the same amount of D₂ adsorbed on the clean Pt surface.

The study of the adsorption of olefins on Pt(111) and its interaction with hydrogen will be reported in a subsequent publication.

Conclusion

1. At temperatures of 110°K alkanes C₄H_{2n+2} with n > 4 adsorbed readily on a Pt(111) surface. The main desorption peaks occurring at 166°K and 195°K for C₄H₁₀ and C₅H₁₂, respectively. Desorption is a first order process with kinetic parameters $\nu = 9.4 \times 10^{10} \text{sec}^{-1}$, E=8.2 kcal/mol, and $\nu = 3.7 \times 10^{11} \text{sec}^{-1}$, E=10.2 kcal/mol for C₄H₁₀ and C₅H₁₂, respectively. Multilayers of hydrocarbons are formed at 110°K for high exposures.

2. The presence of patches of subsurface oxygen gives rise to new adsorption sites of lower binding energy. Saturation of the clean Pt regions and the subsequent formation of multilayers requires lower hydrocarbon exposures in this circumstance.

3. Preadsorbed deuterium interacts repulsively with the adsorbed hydrocarbons, lowering its desorption temperature and resulting in the formation of multilayers at exposures lower than those required on the clean Pt surface. At high deuterium coverages, a more rapid decrease in the binding energy of the hydrocarbon is observed which may be due to its adsorption on D-covered regions.

Acknowledgement:

This work was partially supported by the Spanish-American Cooperation Program which the authors gratefully acknowledge; and by the Director, Office of Energy Research, Office of Basic Energy Sciences, Materials Sciences Division of the U.S. Department of Energy under Contract W-7405-ENG-48.

References

1. G. A. Somorjai, Chemistry in Two Dimensions: Surfaces, Cornell University Press, Ithaca, NY, 1981.
2. L.E. Firment, J.C.P. 66, 2901 (1977).
3. C.M. Chan and W.H. Weinberg, Appl. of Surface Sci. 1, 377 (1978).
4. P.A. Redhead, Vacuum 12, 203 (1962).
5. G. Ehrlich, Adv. Catalysis 14, 255 (1963).
6. D.A. King, Surface Sci. 47, 384 (1975).
7. M. Salmerón and G.A. Somorjai, Surface Sci. (to be published 1981).
8. M. Salmerón and G.A. Somorjai, submitted to J.V.S.T.

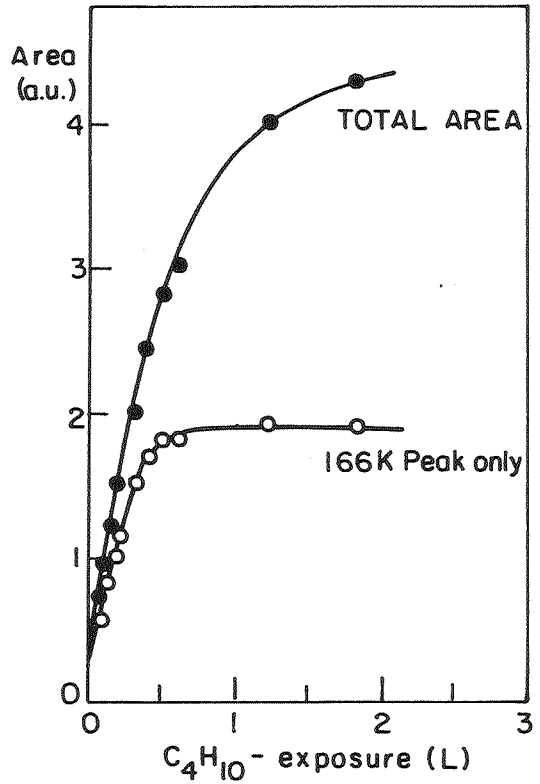
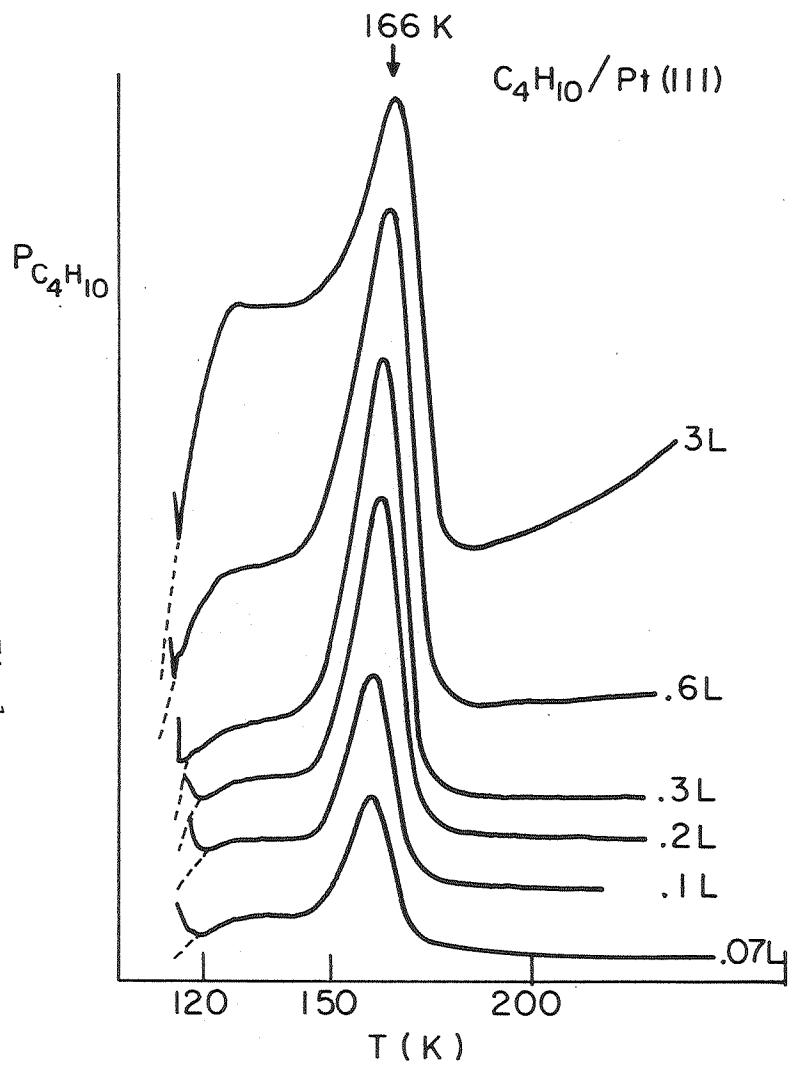
Figure Captions

- Fig.1 Thermal desorption spectra of C_4H_{10} from Pt(111) for various exposures at 110°K. The partial pressure $P_{C_4H_{10}}$ is measured with a mass spectrometer tuned to a mass number of 58. Heating rate is $10^\circ K \text{ sec}^{-1}$. The insert shows the increase of the area under the TDS curves as a function of exposure in Langmuirs (L).
 $1 \text{ L} = 10^{-6} \text{ Torr x sec}$.
- Fig.2 Thermal desorption spectra of C_4H_{10} from a Pt(111) surface containing subsurface oxygen. The curve of points superimposed on the 0.2 L exposure curve corresponds to a preadsorption of 0.5 L of D_2 . The peak at 134°K corresponds to desorption from multilayers. The dashed peak at the lowest temperature corresponds to desorption from the Pt wires' support. It is only shown for the upper curve. The heating is $10^\circ K \text{ sec}^{-1}$. In the insert is shown the increase of the area under the desorption curves versus hydrocarbon exposure.
 $1 \text{ L} = 10^{-6} \text{ Torr x sec}$.
- Fig.3 Thermal desorption spectra of C_5H_{12} from Pt(111) for various exposures. The dashed peak at the lowest temperature is due to desorption from the Pt wires' support. It is shown only in the upper curve. The partial pressure $P_{C_5H_{12}}$ is measured with the mass spectrometer tuned to a mass number of 72. The heating rate is $10^\circ K \text{ sec}^{-1}$. The insert on the right side shows the measured and calculated desorption profile for the kinetic parameters shown. The calculated curve is normalized to the height of the experimental one.
- Fig.4 Area under the desorption curves of C_5H_{12} in arbitrary units versus exposure in Langmuirs ($1 \text{ L} = 10^{-6} \text{ Torr x sec}$). The formation of multilayers ($\theta=1$) corresponds to the appearance of the peak at 125°K in Figure 3.
- Fig.5 Thermal desorption spectra of C_5H_{12} from an oxygen treated Pt(111) surface. Heating rate $8^\circ K \text{ sec}^{-1}$. The dashed peak corresponds to desorption from the Pt wires' support and is only shown for the upper curve.
- Fig.6 Area under the D_2 thermal desorption curves as a function of D_2 exposure on Pt(111) at 110°K. The value of $\theta=1$ is assigned to the extrapolated saturation which corresponds to an area of 4 in the units of the graphic.

Fig.7 Thermal desorption spectra from C_5H_{12} adsorbed on a Pt(111) surface previously exposed to D_2 . The C_5H_{12} exposure is 0.1 L (1 L= 10^{-6} Torr x sec). The exposure of D_2 is indicated on the right side of each curve.

Fig.8 Activation energy and peak temperatures for desorption of C_6H_{12} from a Pt(111) surface precovered with various amounts of deuterium. The shift in temperature of the 195°K peak (for $\theta_D=0$) is similar for two hydrocarbon exposures.

Fig. 1



XBL 814-5467

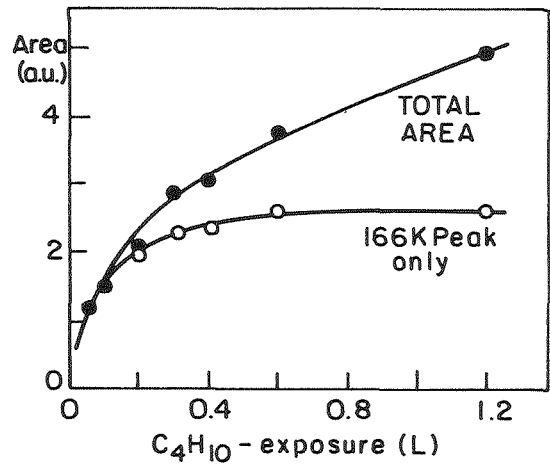
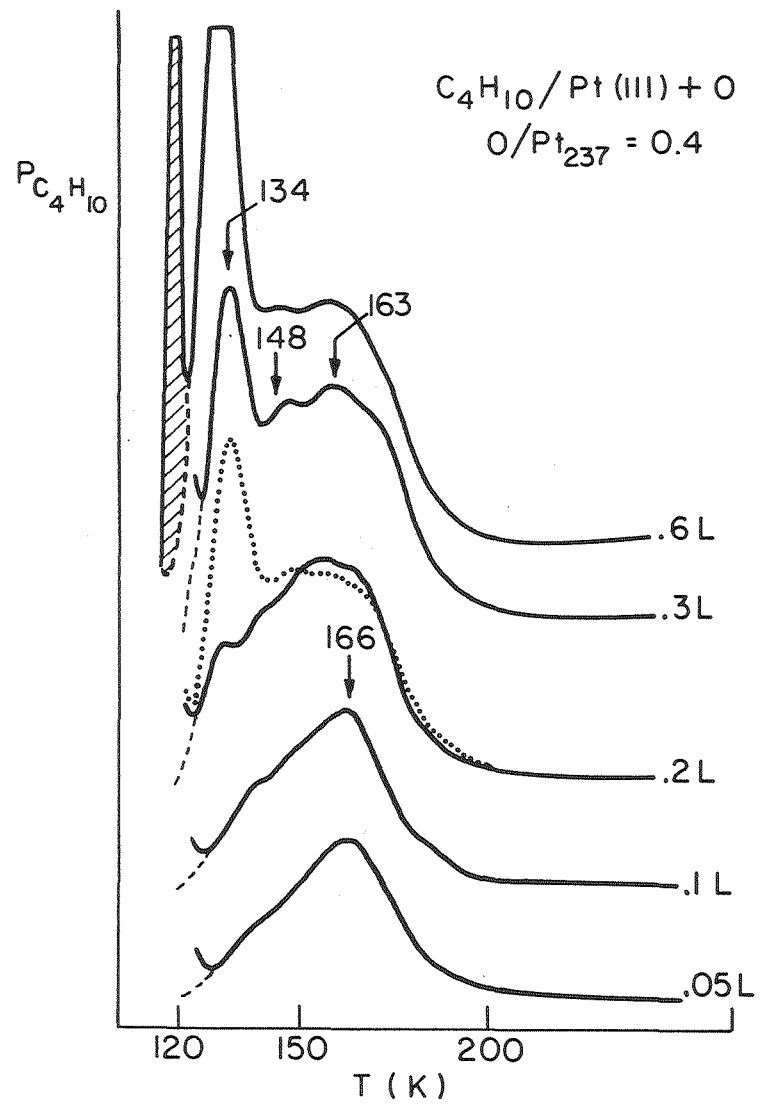
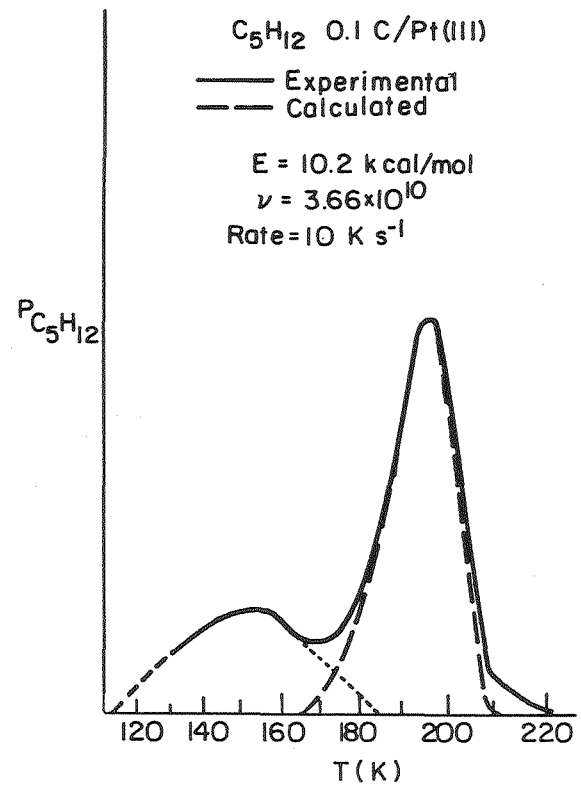
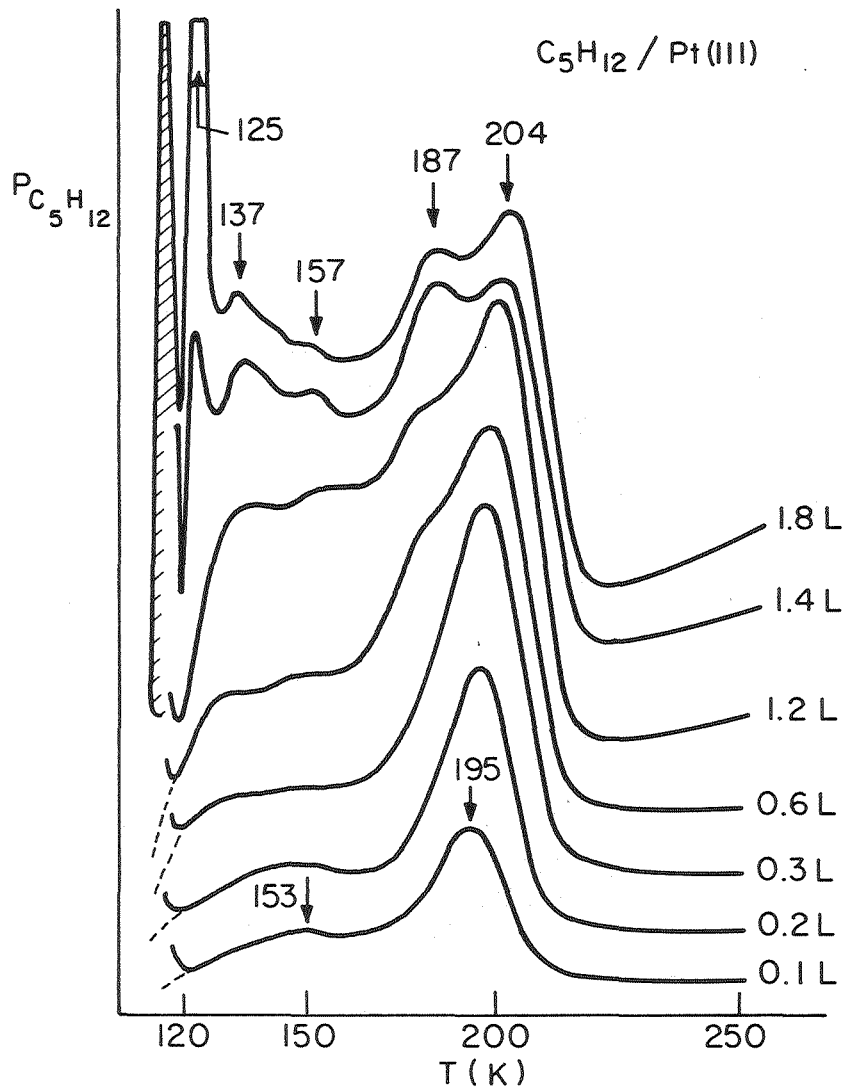


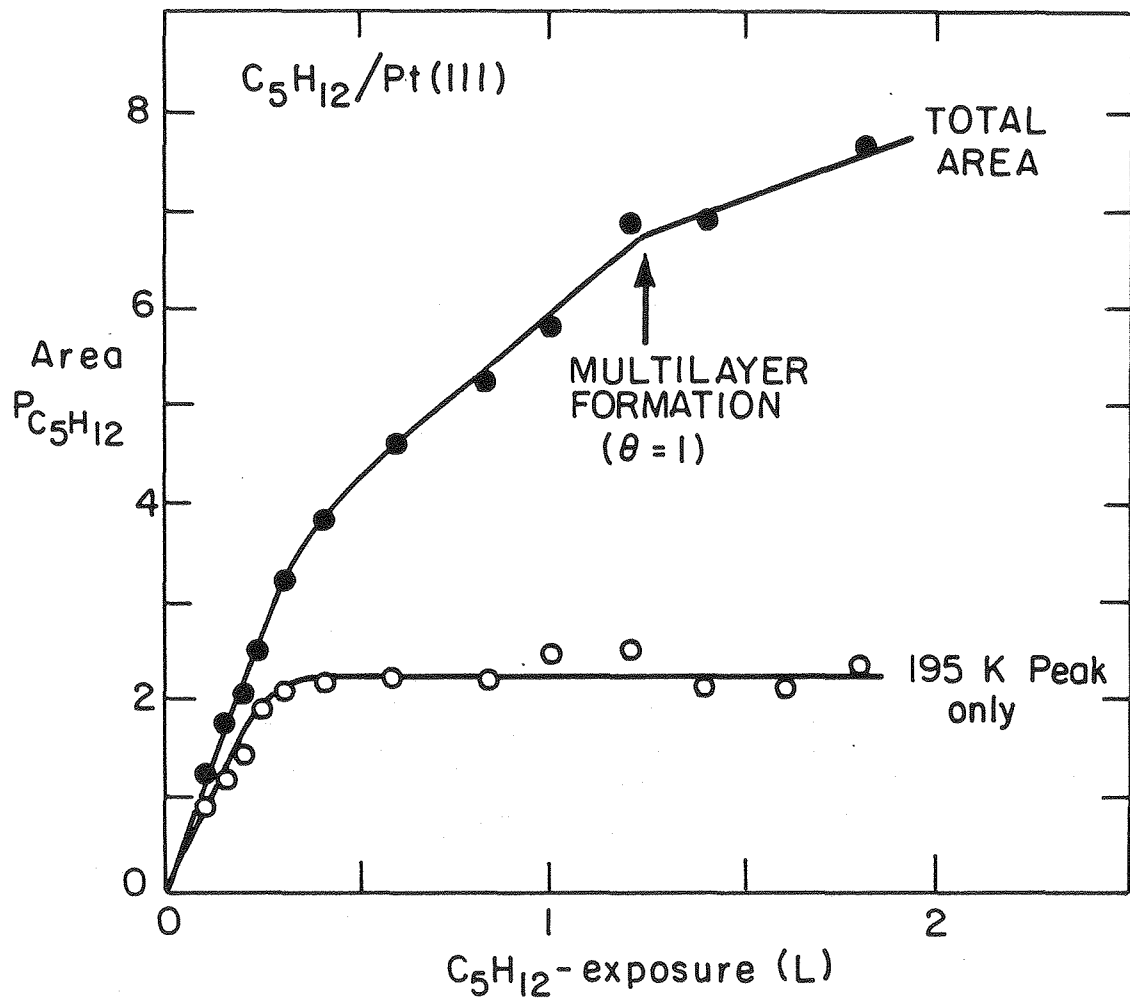
Fig. 2

XBL 814-5468

Fig. 3

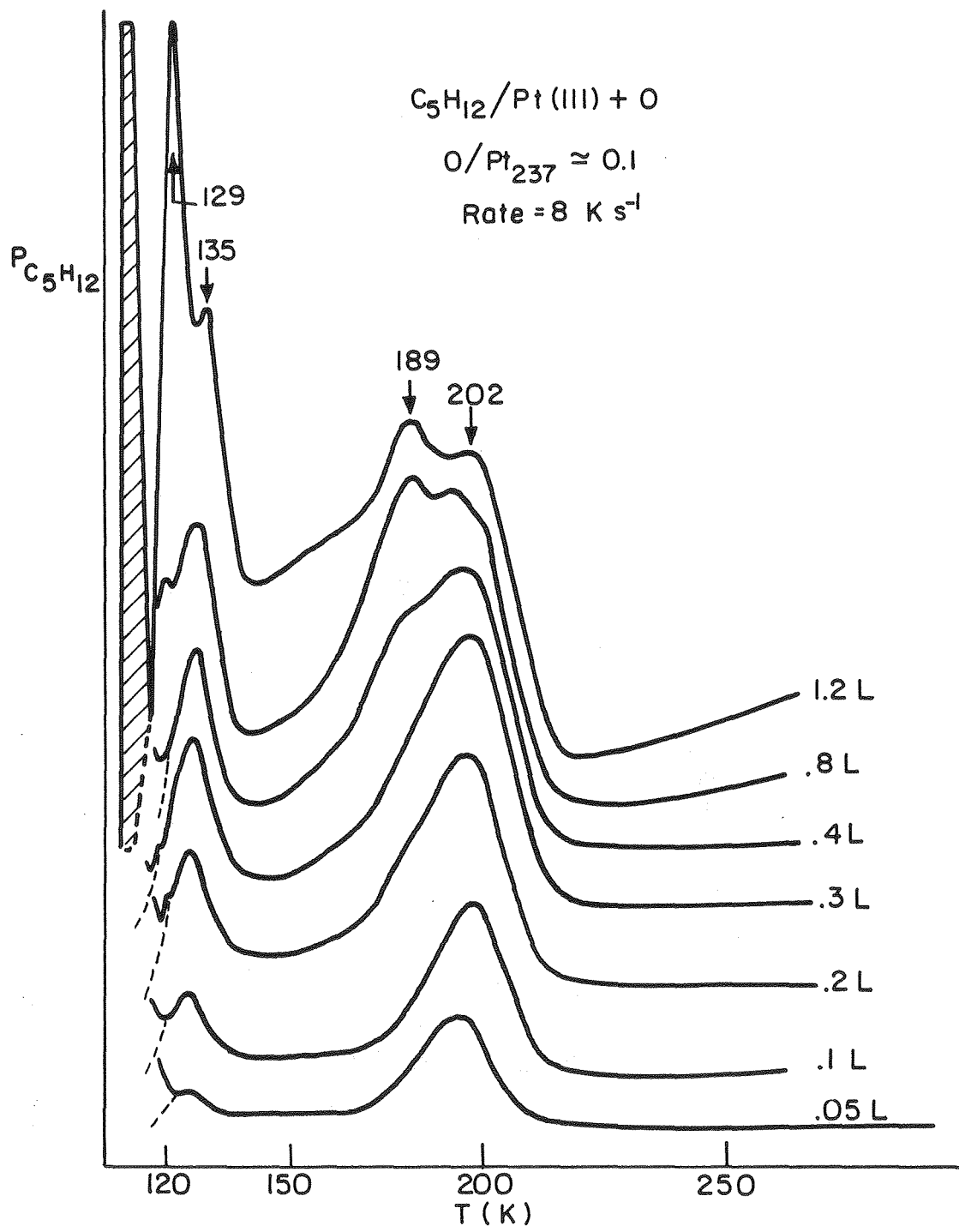


XBL814-5469



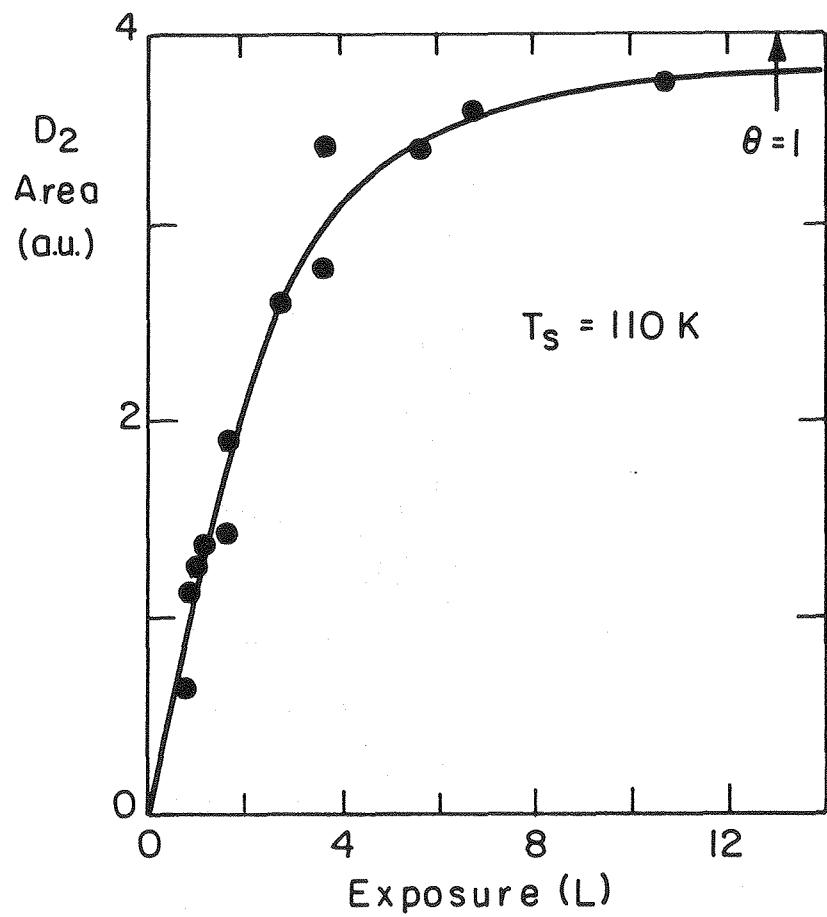
XBL814-5470

Fig.4



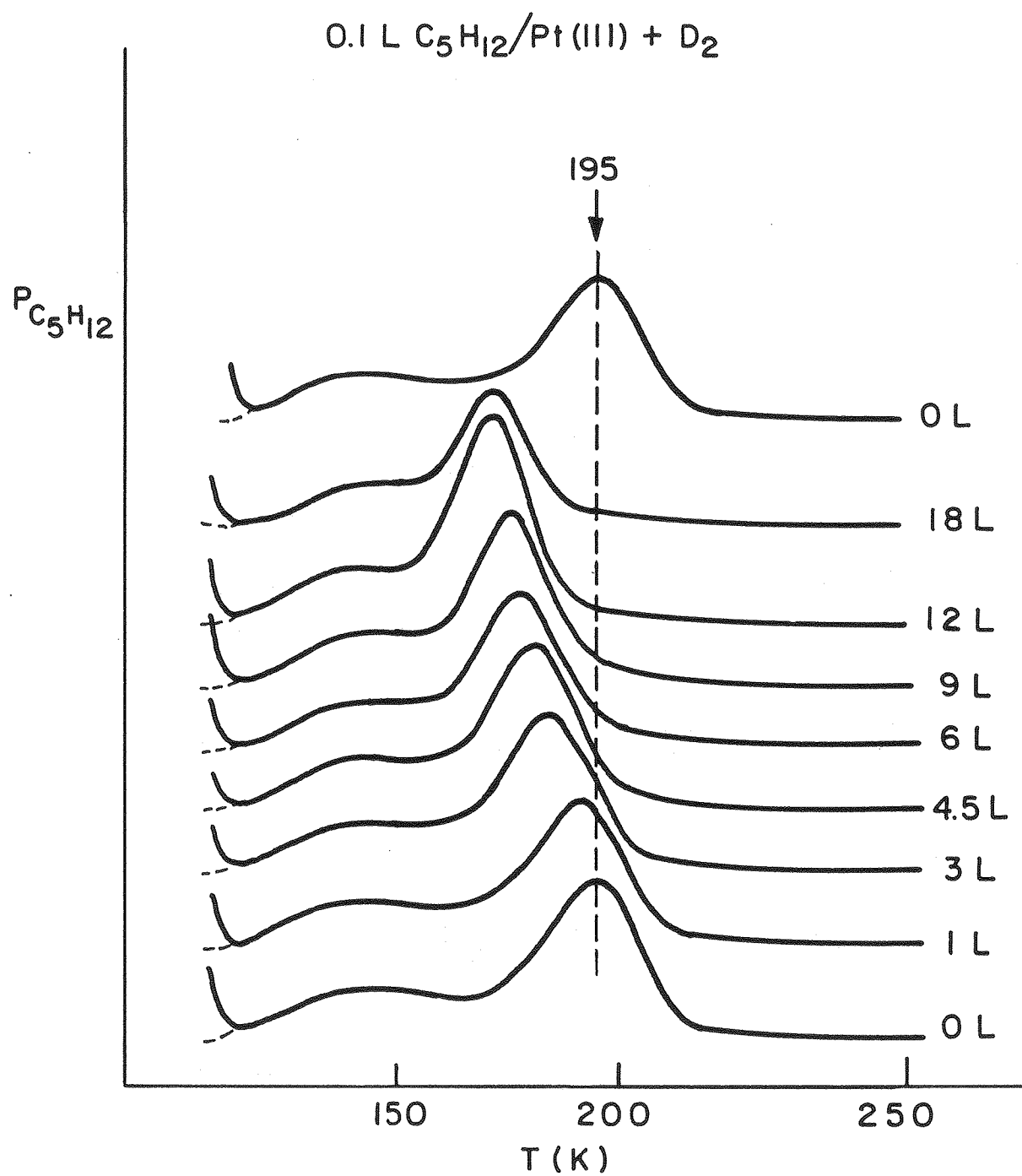
XBL 814-5471

Fig.5



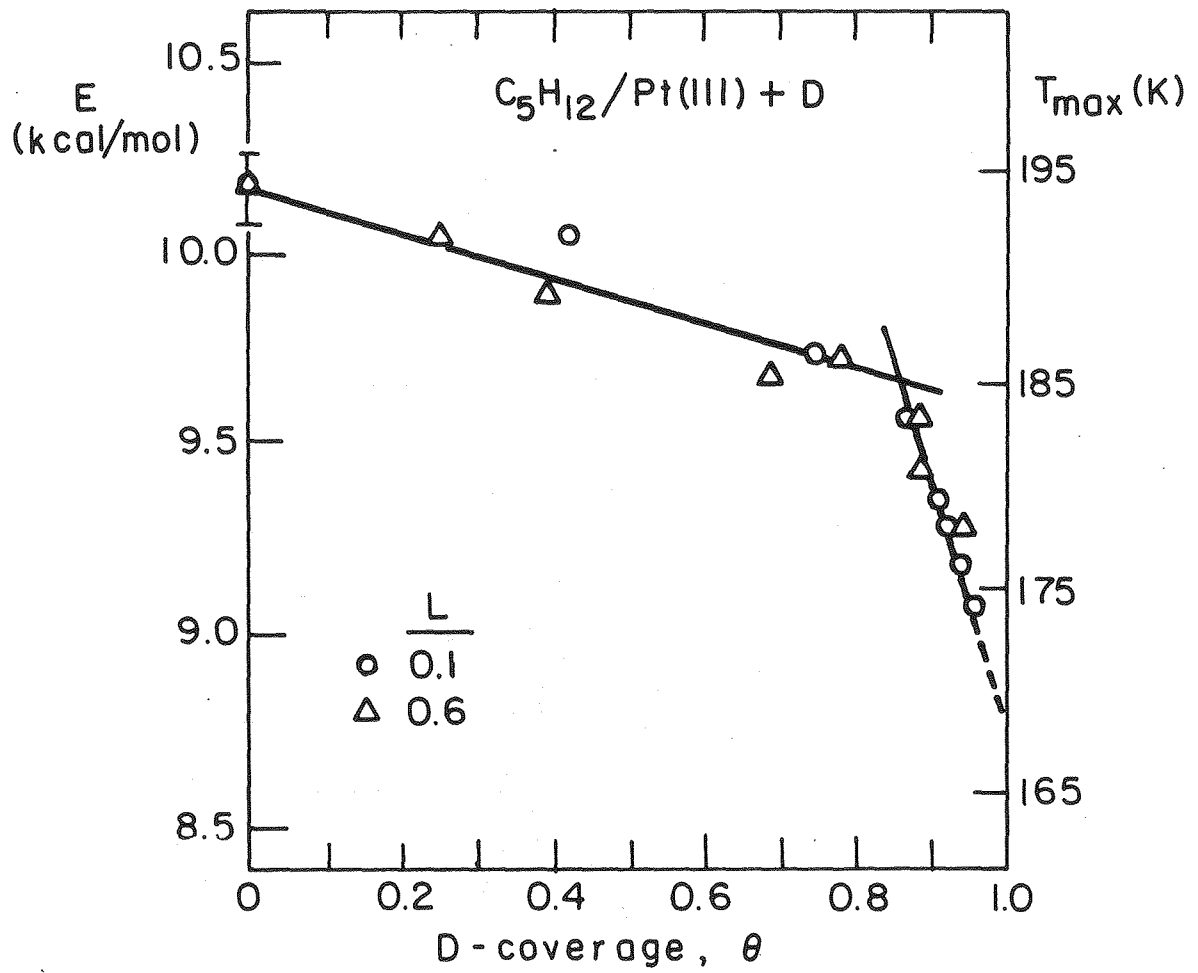
XBL 814-5472

Fig.6



XBL 814-5473

Fig.7



XBL 814-5474

Fig. 8